General Paper

Analyses of Influence of Frictional Heat on the Contact Stress of High-speed Micro-gears

Cheol Kim*†, **Hyeong-Seok Kim***

ABSTRACT: When a small gear rotates at a very high speed over 40,000 rpm, frictional heat is generated on the gear surfaces. Thermal deformations and stresses arising from frictional heat may lower the efficiency and fatigue life of the high-speed gear. Especially, such frictional heat has much stronger effects on the performance of millimeter-sized high-speed gears used for surgical and dental hand-pieces, due to a small surface area. An analytical equation was derived to calculate frictional temperature on a mating gear surface and conduction heat transfer analysis was performed. Thermal deformation and contact stresses were then calculated using FEM for gears used for medical hand-pieces. The contact stresses of the meshed gear and pinion increase by 19.4% and 16.4%, respectively, when the frictional thermal deformations are considered.

Key Words: Contact stress, Friction heat, Surgical handpiece, Gear, Steel alloy

1. INTRODUCTION

Small surgical gear-type hand-piece is used to cut diseased biological tissues out in a medical operation and consists of a small driving BLDC motor, a small high speed gear train and a small knife or a saw at the tip. Mating gears of a hand-piece usually rotate at over 40,000 rpm in order to transfer power to an end knife or saw by way of cams or any other motion-changing devices. High speed revolution naturally causes high frictional heat on the contacting gear surfaces and causes thermal strains in gears. Excessive thermal strains may have a detrimental effect on the fatigue strength of gears and cause vibrating noise.

Fatigue analysis was performed for the surface of gear teeth flanks by FEM [1] and surface contact stresses were computed in an effort to enhance the surface fatigue life [2-5]. Fatigue failure of a helical gear in a gearbox was investigated in order to design an automotive transmission [6]. Residual stresses were also analyzed in the region of peened gear surfaces [7,8]. A physics-based model was recently developed to predict the micro-pitting behavior on contact surfaces of spur gears operating under the mixed lubrication condition [9]. Tooth tem-
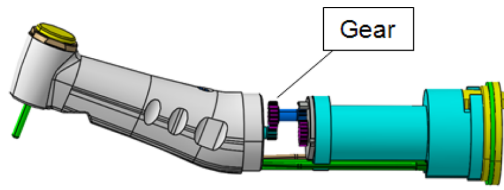
perature analysis of a spur gear was performed using the FEM with calculation of heat input and estimation of heat transfer coefficients as well as experimental measurements using the infrared radiometric microscope [10]. A numerical and analytical study including gear dynamic load, lubricant film thickness, bulk equilibrium and total flash temperatures in spur gear contacts was reported by Wang and Cheng [11]. The distribution of bulk equilibrium temperature and flash temperature along the contact path for pinion and gear teeth were derived and the influences of face width, outside radius and pitch diameter were evaluated [12]. Long *et al.* [13] investigated the effects of gear geometry, rotational speed and applied load, as well as lubrication conditions on surface temperature of medium-speed (up to 10,000 rpm) gear teeth.

However, there are little studies on the high speed small millimeter-sized gears used for various surgical hand-pieces for a medical operation, even though much frictional heat is generated on the contacting surfaces of meshed gears. In this study, the contact stress, thermal strains and stresses in the meshed gears of a surgical hand-piece were computed using ABAQUS finite element analysis. The contact stresses including a thermal effect were compared with those excluding it in
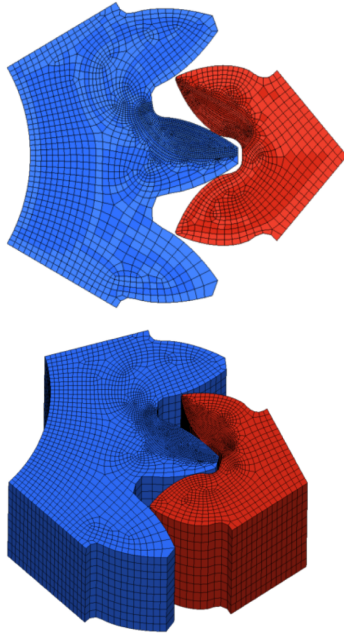
(a) A small gear-driven medical hand-piece

(b) A gear section for analysis (the left is a gear and the right is a pinion)

Fig. 1. A hand-piece and a finite element model of mating gear segments

Table 1. Specifications of gears

Parameters	Gear	Pinion
Number of teeth (N)	18	8
Module (m) [= pitch dia. / N]	0.25	
Pressure angle [deg.]	20	
Circular pitch (p)	0.7854	
rpm	40,000	90,000

Table 2. Material properties of SUS420F for gears [14]

Density [kg/mm^3]	7.8×10^{-6}
Modulus of elasticity [GPa]	200
Poisson's ratio	0.24
Thermal expansion coeff. [m/m·$^\circ$C]	10.3×10^{-6}
Thermal conductivity [W/m·K]	24.9
Specific heat [J/g·$^\circ$C]	0.460

Fig. 2. Contact stress distribution during the rotation of meshed gears ("pinion" with a sharp top)

Table 3. Finite element meshes

Info.	Gear	Pinion
No. of finite elements (C3D8)	29,480	18,730
No. of nodes	33,550	21,505

order to assess the change in contact strength.

2. CONTACT ANALYSIS

The mating gears are modeled with ABAQUS 3-D 8-noded HEXA elements (C3D8) to analyze contact stresses, as in Fig. 1. Three gear teeth and two pinion teeth were included in the FE model in order to capture surface contact stresses, bending stresses and thermal stresses accurately. The contact region was finely meshed and the contact condition of ABAQUS was applied. The specifications of gear and pinion are listed in Table 1. The force of one tooth pushing against the other is always transmitted at the pressure angle (usually, 20 or 25 degree). All nodes on the cross-section of a pinion FE model were fixed and a torque of 20.5 N-mm transferred from a BLDC motor was applied for a gear using rigid bar elements. Both a gear and a pinion were fabricated with martensite stainless steel alloy (C, Si, Mn, P, S, Cr, Ni, Mo) and thermal and material properties are tabulated in Table 2. The distribution of contact stresses is plotted in Fig. 2. The maximum
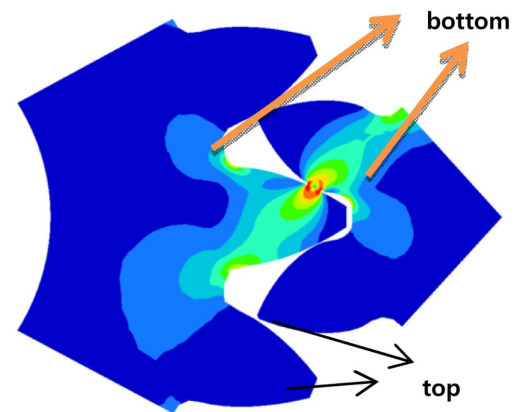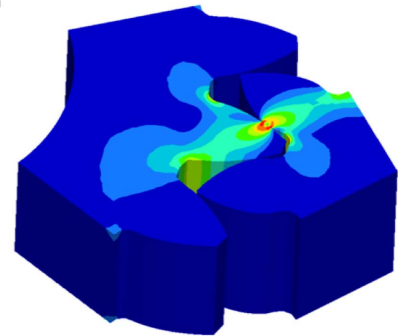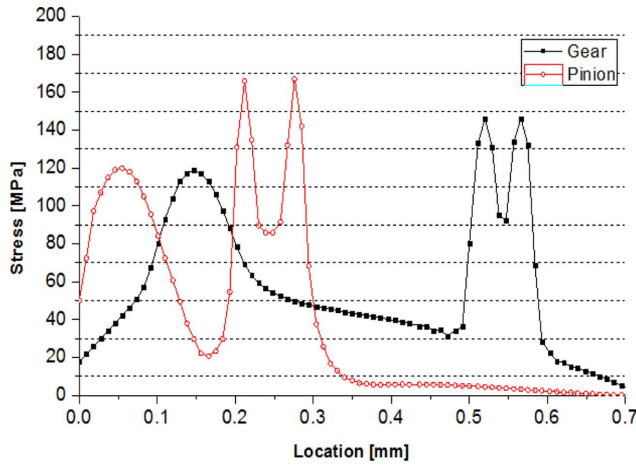
Fig. 3. Contact stresses along the gear surface from a tooth bottom (0.0 mm) to an end (0.7 mm) at the contact position in Fig. 2

stress of 167.7 MPa was obtained at the pinion around the contact point. The numbers of finite elements and nodes are listed in Table 3.

Fig. 3 shows the contact stress distribution along a contacting surface from a tooth bottom (0.0 mm) and a top (0.7 mm) of gear and pinion at the position described in Fig. 2. The origin of a coordinate in Fig. 3 is set on a point of a tooth bottom area. The contact stress in the pinion is higher than that in the gear. The stresses in the teeth roots of two gears are similar each other and 120 MPa. The sharp peaks of gear and pinion in Fig. 3 occurred actually around the contact point even though the two are apart due to a different distance from the tooth bottom. The maximum stress is 146.2 MPa in a gear and 167.7 MPa in a pinion, as in Fig. 3.
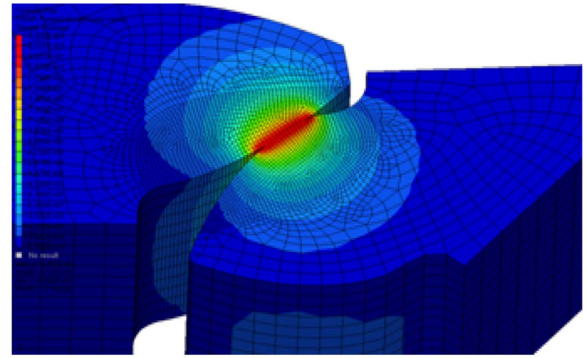
3. THERMAL ANALYSIS

It is important to evaluate the influence of thermal stress on the contact area because the small high-speed mating gears (40,000–90,000 rpm) generate naturally much frictional heat on gear surfaces. The diameter of a spur gear for a surgical hand-piece is 3.2 mm small. It is difficult to measure the surface temperature of gears due to the small height of a tooth, 0.7 mm and a high angular speed over 40,000 rpm. An equation which can predict the frictional surface temperature was derived on the basis of an AGMA gear theory [15] as follows,
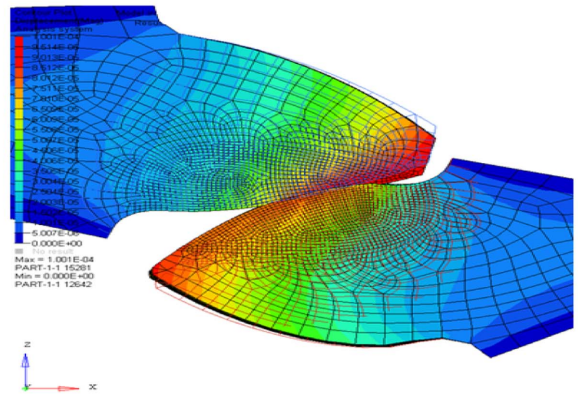
$$H_d = hA_s(T_s - T_\infty) = (HP)_{loss} \tag{1}$$

$$(HP)_{loss} = (1-e)(HP)_i = \left[1 - \frac{(HP)_o}{(HP)_i}\right](HP)_i \tag{2}$$

$$e = 1 - \varepsilon\mu\pi\left(\frac{1}{z_1} - \frac{1}{z_2}\right) \tag{3}$$

(a) Heat transfer from a contact surface toward inside

(b) Thermal strain distribution during rotation

Fig. 4. Heat conduction from the surface and thermal strain distribution while gears rotate (an upper tooth is a gear and lower one is a pinion)

$$A_s = [(r_p + a_p) - (r_p\cos\Phi)^2]^{1/2} + [(r_g + a_g) - (r_g\cos\Phi)^2]^{1/2}$$
$$- c\sin\Phi \tag{4}$$

$$(HP)_i = \frac{Tn}{9.549} \tag{5}$$

where H_d represents the time rate of heat dissipation and h is a local convection coefficient. As is a contact surface area of a gear tooth, T_∞ is an ambient temperature, T_s is a temperature on a tooth surface, and $(HP)_{loss}$ denotes loss of horsepower (HP). The quantity e represents the efficiency. The subscripts, i and o, denote input and output, respectively. The quantity ε represents a contact ratio and μ is a friction coefficient (0.026). z_1 and z_2 are the number of gear and pinion teeth, respectively. The quantities, r, a, c and Φ, are a pitch radius, an addendum, a center distance between two gears, and a pressure angle, respectively and the subscripts, p and g, denote a pinion and a gear, respectively. The horsepower input in Eq. (2), $(HP)_i$, can be expressed in terms of a torque (T) and rpm (n) as in Eq. (5).

From Eqs. (1)-(5), an equation for a frictional surface temperature on a gear tooth which rotates in a high speed is obtained as follows,
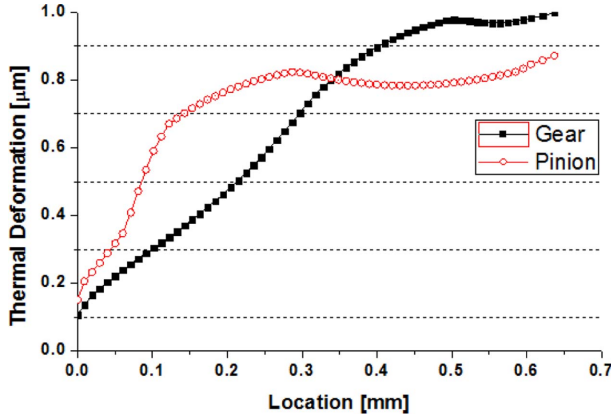
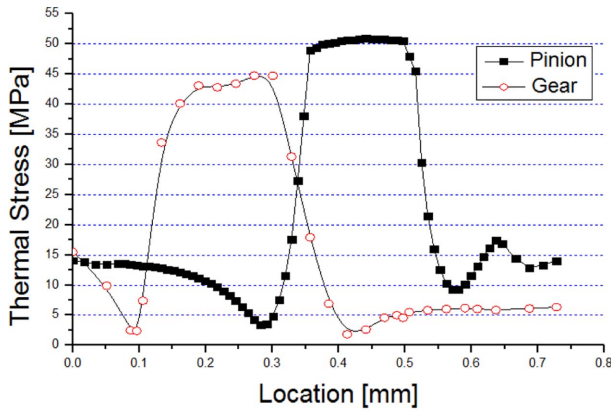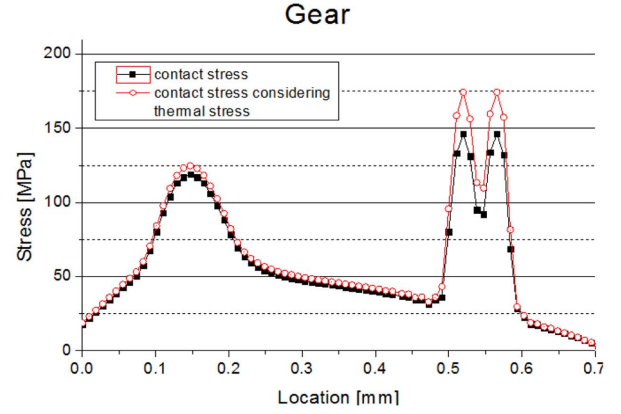**Fig. 5.** Thermal deformations on surfaces of the meshed gear and pinion

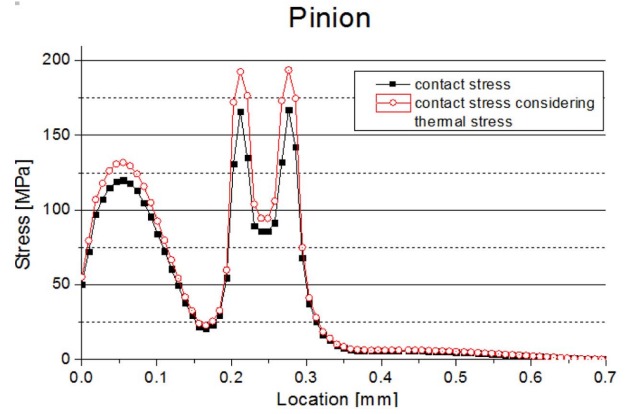**Fig. 6.** Thermal stress (von Mises) distribution on the surface of a mating gear tooth

(a) Gear

(b) Pinion

Fig. 7. The contact stress distribution with and without the effect of frictional heat for a gear (a) and a pinion (b)

$$T_s = (1-e)\frac{Tn}{9.549}\frac{1}{hA_s} + T_\infty \qquad (6)$$

An initial temperature on the gear surface was set to be 26.6°C and an ambient temperature around gears inside the hand-piece was measured to be 55°C. The convection coefficient (h) was assumed to be 270 W/m^2·°C from numerical experiments. The BLDC motor torque measured is 20.5 N-mm. The resulting surface temperature of 82.85°C was calculated at the contact surface from the Eq. (6). Based on the calculated surface temperature of 82.85°C, the temperature distribution by heat conduction was computed with ABAQUS finite element (C3D8T) analyses as in Fig. 4(a) and thermal strains during rotation were computed as in Fig. 4(b).

Because the thermal deformations of small high-speed gears due to frictional heat may cause changes in a contact ratio, unsmooth rotation and efficiency loss, they were computed based on the results of heat transfer analysis, as in Fig. 4(b). Fig. 5 shows the distribution of thermal strains on the surfaces of the mating gear and pinion. The origin of the graph was set to be at the bottom of meshed gear teeth. Thermal deforma-

tions are in the range of 0.1 to 1.0 μm and the largest occurs at the end of a tooth, as shown in Fig. 5. Considering that the height of a tooth is 0.7 mm, the thermal deformation of 1.0 μm is not small. Therefore, a relevant cooling system must be accompanied. The thermal stress distribution due to the frictional heat generation is plotted in Fig. 6. The maximum thermal stresses of 50.9 MPa and 46.2 MPa occurred naturally on the contact surface of the pinion and the gear as in Fig. 6, respectively.

4. CONTACT STRESS CONSIDERING FRICTIONAL HEAT

Now, contact stresses are computed with the finite element analysis considering the torque transfer and the thermal deformations simultaneously. In the previous section, we noticed that thermal deformation itself due to teeth frictional heat exerted an unfavorable influence on contact stresses. Figs. 7 and 8 represent the distribution of contact stresses (von Mises) in the meshed gear and pinion when thermal and mechanical strains are considered simultaneously.
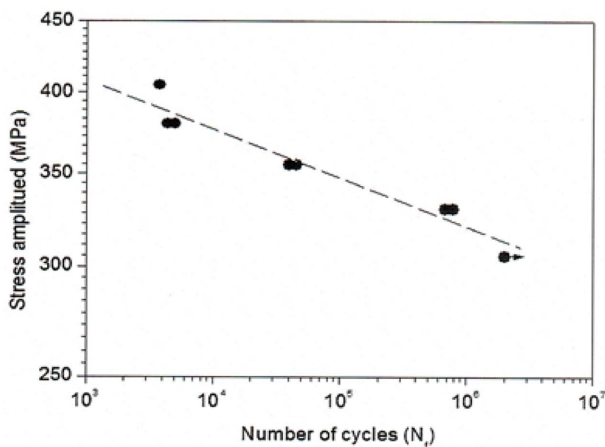
Fig. 8. The S-N curve of SUS420F gear material obtained by fatigue tests

As for a gear, maximum von Mises stress due to a torque transfer is 146.2 MPa in the contact area and the contact stress due to torque transfer and thermal deformation is 174.5 MPa. As for a pinion, maximum von Mises stress due to a torque transfer is 167.7 MPa in the contact area and the contact stress due to torque transfer and thermal deformation is 195.2 MPa. The contact stresses of the meshed gear and pinion increase by 19.4% and 16.4%, respectively, when the frictional thermal deformations are included. These additional contact stresses may significantly reduce the fatigue life of a small high-speed gear. To cope with frictional heat, an effective cooling system using water or oil is required.

The S-N curve was determined experimentally for this study, as in Fig. 8 and the stresses due to torque transfer and thermal deformation are under endurance limit by fatigue testing.

5. CONCLUSIONS

The thermal stresses arising from the frictional heat of millimeter-sized high-speed gears (40,000-90,000 rpm) in a surgical or dental hand-piece may lower the efficiency and a fatigue life of the mating high speed gear. A new equation which can predict the frictional surface temperature of meshed rotating small gears was developed on the basis of a torque, rpm, efficiency and heat conduction. Thermal deformations and contact stresses of mating gears were calculated using nonlinear finite element analysis. The contact stresses of the meshed gear and pinion increase by 19.4% and 16.4%, respectively, when the frictional thermal deformations are considered. It is quantitatively proved that gear frictional heat has a strong influence on contact stresses between meshed high speed gears.

REFERENCES

1. Glodez, S., Ren, Z., and Flasker, J., "Surface Fatigue of Gear Teeth Flanks," *Computers & Structures*, Vol. 73, No. 1, 1999, pp. 475-483.
2. Kim, C.H., Ahn, H.S., and Chong, T.H., "On a Method for the Durability Enhancement of Plastic Spur Gear Using Finite Element Analysis," *Trans. of KSME (A)*, Vol. 27, No. 2, 2003, pp. 223-230.
3. Chen, Y.C. and Tsay, C.B., "Stress Analysis of a Helical Gear Set with Localized Bearing Contact," *Finite Element in Analysis and Design*, Vol. 38, No. 8, 2002, pp. 707-723.
4. Guagliano, M., Riva, E., and Guidetti, M., "Contact Fatigue Failure Analysis of Shot-peened Gears," *Engineering Failure Analysis*, Vol. 9, No. 2, 2002, pp. 147-158.
5. Hwang, S.C., Lee, D.H., Park Y.C., and Lee, K.H., "Contact Stress Analysis of Helical Gear for Turbo Blower," *J. of KSMPE*, Vol. 10, No. 2, 2011, pp. 90-95.
6. Asi, O., "Fatigue Failure of a Helical Gear in a Gearbox," *Engineering Failure Analysis*, Vol. 13, No. 7, 2006, pp. 1116-1125.
7. Wang, J., Wang, Y., and Huo, Z., "Finite Element Residual Stress Analysis of Planetary Gear Tooth," *Advances in Mech. Eng.*, Vol. 2013, 2013.
8. Lee, D.S., Lee, K.J., Kim, T.H., Hwang, J.H., Lee, J.H., and Cheong, S.K., "Investigation of Optimal Peening Intensity of Gear with Stress Concentration for Improvement of Fatigue Life," *Proc. of the KSME 2005 Annual Conf., Pyeongchang*, Korea, Nov. 2005, pp. 1341-1346.
9. Li, S. and Kahraman, A., "A Micro-pitting Model for Spur Gear Contacts," *International Journal of Fatigue*, Vol. 59 2014, pp. 224-233.
10. Townsend, D.P. and Akin, L.S., "Analytical and Experimental Spur Gear Tooth Temperature as Affected by Operating Variables," *J. Mech. Design.*, Vol. 103, No. 1, 1981, pp. 219-226.
11. Wang, K.L. and Cheng, H.S., "A Numerical Solution to the Dynamic Load, Film Thickness and Surface Temperatures in Spur Gears," *Part I: Analysis, J. Mech. Design.*, Vol. 103, No. 1, 1981, pp. 177-187.
12. Wang, K.L. and Cheng, H.S., "A Numerical Solution to the Dynamic Load, Film Thickness and Surface Temperatures in Spur Gears," *Part II: Results, J. Mech. Design.*, Vol. 103, No. 1, 1981, pp. 188-194.
13. Long, H., Lord, A.A., Gethin, D.T., and Roylance, B.J., "Operating Temperatures of Oil-lubricated Medium-speed Gears: Numerical Models and Experimental Results," *Proc. Instn. Mech. Engrs. Part G: J. Aerospace Engr.*, Vol. 217, No. 2, 2003, pp. 87-106.
14. http://www.matweb.com/
15. Shigley, J.E., Mischke, C.R., and Budynas, R.G.., *Mechanical Engineering Design*, pp. 797-804 McGraw Hill, Singapore, 2004.